

Verification of Newton's Laws Using an Airtrack Lab Report 1

Ayaan Dutt
Lab partner: Raheem Manoj

Professor Susmita Saha
TAs: Spandan Pandya, Shwetha Prakash
TF: Samrat Roy

Date of Experiment: August 29th, 2023

Date of Submission: September 12th, 2023

Aim

- Verify Newton's first law by observing the velocity of a mass with no external force acting on it.
- Verify Newton's second law by observing the acceleration of a mass with a constant force acting on it.
- Verify Newton's third law by observing the momentum of two masses undergoing an elastic collision.

Experimental Setup

- A 2-metre long air track.
- A blower to pump air into the track.
- End attachments: steel springs and pulley
- Thin string
- 2 long riders weighing 400g each.
- 1 short rider weighing 200g.
- Several small masses weighing 1g to 15g.
- Long and short interrupter cards to attach onto the riders.
- Attachments to hold rubber bands (for elastic collisions) and their counterweights.
- Attachments with double sided tape (for inelastic collisions) and their counterweights.
- Two vernier photogates with associated their cables and a LabQuest interface.
- A computer with Logger Pro 3 software.

Least count of measuring tape = 0.1 cm
 Least count of weighing scale = 0.1 g

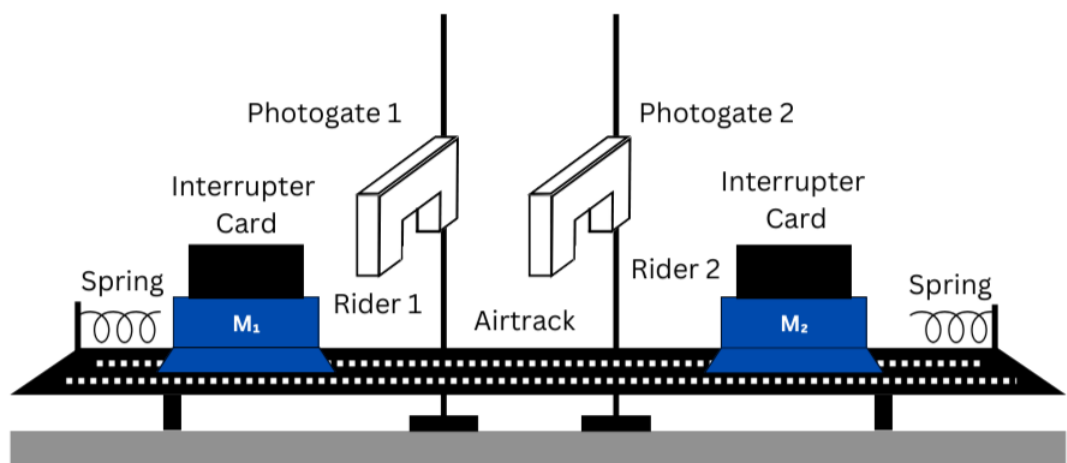
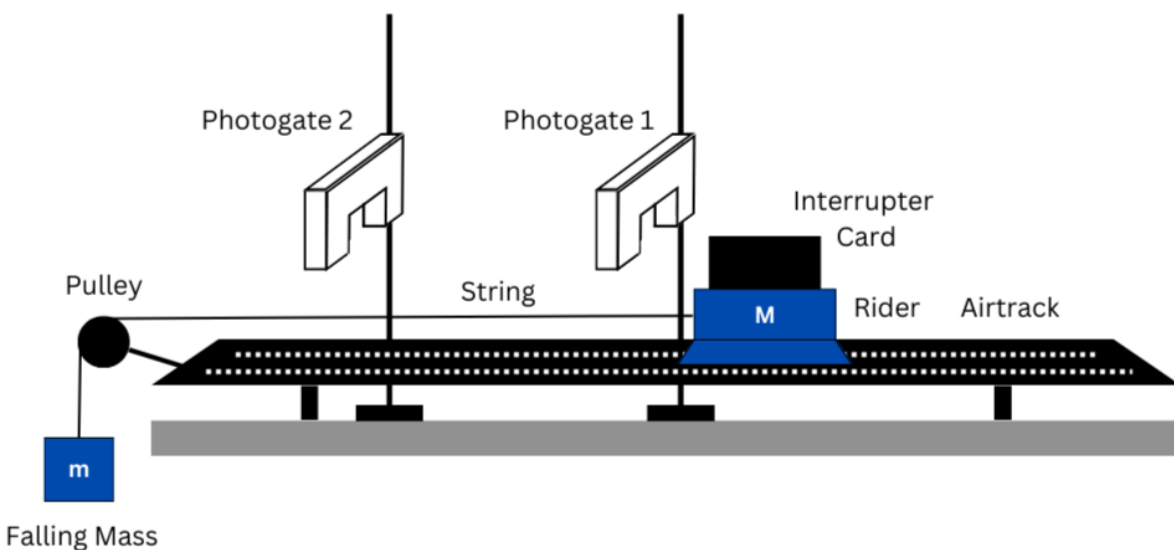
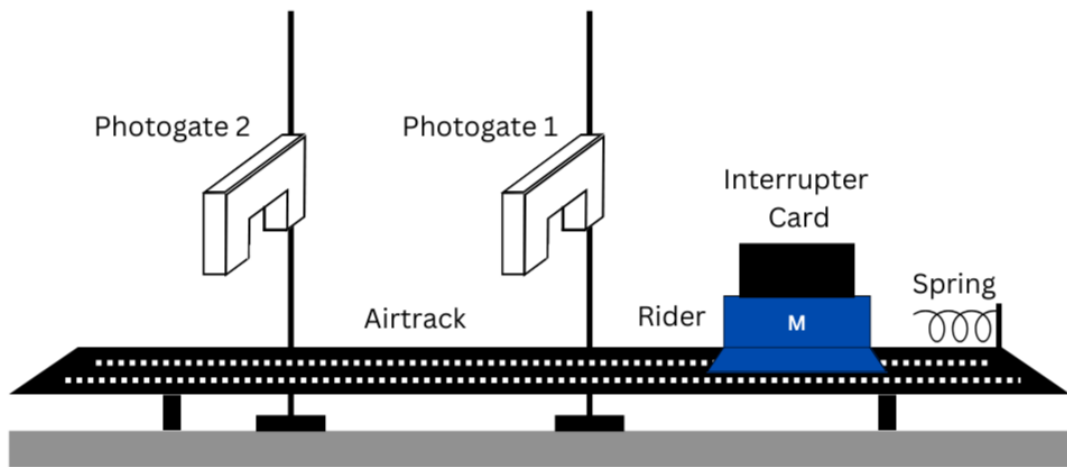


Figure 1: Experimental setup of the verification of Newton's laws using an airtrack for part A, B and C, from top to bottom, respectively

Theoretical Background

Part A

Newton's first law of motion, often referred to as the law of inertia, states that an object at rest will remain at rest, and an object in motion will remain in uniform rectilinear motion unless acted upon by an external force.

This can be experimentally verified by showing that the velocity of a body released from a spring on a nearly friction-less airtrack remains constant between two different points in its trajectory.

Assuming an ideal spring, the potential energy stored in its compressed state is $U = \frac{1}{2}kx^2$ for a spring compression x . This energy is completely converted into kinetic energy of the rider $T = \frac{1}{2}mv_0^2$. Equating the two, we get:

$$\begin{aligned}\frac{1}{2}kx^2 &= \frac{1}{2}mv_0^2 \\ v_0 &= x\sqrt{\frac{k}{m}}\end{aligned}\tag{1}$$

Part B

Newton's second law states that under a constant force, a body moves with a constant acceleration. The mass of the body times its acceleration is equal to the net external force on the body.

$$F_{ext} = ma$$

For the experimental setup of a falling mass attached to the rider via a pulley, we can draw the following free body diagram.

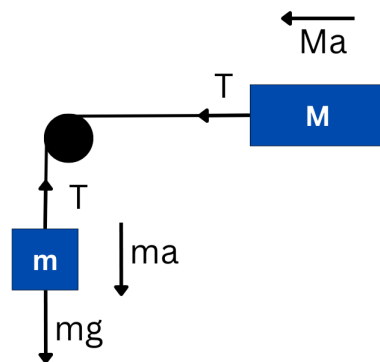


Figure 2: Free body diagram of the falling mass (m) and rider (M)

From fig 2 we can get the following equations:

$$Ma = T$$

$$ma = mg - T$$

Combining the above equations, we get the relation:

$$a = \frac{mg}{m + M}\tag{2}$$

Part C

Newton's third law of motion states that when a body exerts a force on another body, it experiences an equal and opposite force from the other body.

$$F_{12} = -F_{21}$$

Assuming the force acts over a short time interval Δt , the impulse experienced by both bodies must also be equal and opposite:

$$\begin{aligned} F_{12}\Delta t &= -F_{21}\Delta t \\ \implies m_1\Delta v_1 &= m_2\Delta v_2 \\ \implies m_1(v'_1 - v_1) &= m_2(v_2 - v'_2) \end{aligned}$$

This implies that the momentum of the system is conserved before and after the collision:

$$m_1v_1 + m_2v_2 = m_1v'_1 + m_2v'_2 \quad (3)$$

Collisions can be categorized as elastic and inelastic collisions based on whether or not kinetic energy is conserved before and after the collision.

For perfectly elastic collisions where the masses collide and move away with velocities v'_1 and v'_2 :

$$\begin{aligned} m_1v_1 + m_2v_2 &= m_1v'_1 + m_2v'_2 \\ \frac{1}{2}m_1v_1^2 + \frac{1}{2}m_2v_2^2 &= \frac{1}{2}m_1v'_1^2 + \frac{1}{2}m_2v'_2^2 \end{aligned}$$

For perfectly inelastic collisions where the masses collide and stick together, moving with a combined velocity V :

$$\begin{aligned} m_1v_1 + m_2v_2 &= (m_1 + m_2)V \\ \frac{1}{2}m_1v_1^2 + \frac{1}{2}m_2v_2^2 &= \frac{1}{2}(m_1 + m_2)V^2 + \Delta E \end{aligned}$$

Where ΔE is the loss in kinetic energy during a perfectly inelastic collision. This quantity can be found by rearranging the above equations:

$$\Delta E = \frac{1}{2} \left(\frac{1}{\frac{1}{m_1} + \frac{1}{m_2}} \right) (v_2 - v_1)^2 = \frac{1}{2}\mu(v_2 - v_1)^2 \quad (4)$$

Here μ is a quantity known as the reduced mass of the system and is dependent on the colliding masses.

These laws can be verified by checking that the momentum of the riders on a friction-less airtrack is conserved before and after they collide, (elastically and inelastically). Furthermore, the loss of kinetic energy can be found in each case and compared with the theoretically expected value.

Procedure

Part A

- Put springs at either end of the air track. Place a rider at one end of the track, gently push it against the spring. Make note of the compression (l) of the spring before releasing it (Fig 1(a)).
[Precaution: Ensure that the track is levelled and the airflow is uniform to reduce error.]
- Measure the time it takes for the rider to pass a photogate at two different points in its trajectory.
[Precaution: Avoid small spring compressions since low initial velocities are more sensitive to frictional error.]

3. Measure the length of the interrupter card (Δx) on the rider and divide it with the passage time (Δt) at each gate to get two velocity readings per run.
4. Repeat this for different initial velocities.
5. Plot the velocities against the compression of the spring.

Part B

1. Connect a pulley to one end of the airtrack. Pass a thin long string across the pulley and connect it to the rider at one end, and a small mass at the other (Fig 1(b)). *[Precaution: Use a thin light string. Periodically remove any twists to ensure smooth rolling over the pulley and minimize energy loss]*
2. Attach different masses to the string and measure the change in velocity between two points along the riders trajectory to determine the acceleration.
3. Plot the acceleration of the rider against the mass dropped. Use equation 2 to determine the value of g.

Part C

1. Put the steel spring at both ends of the air track, and attach two rubber band attachments (and counterweights) to the riders to simulate elastic collisions.
2. Measure and note the mass of each of the riders with their attachments.
3. Place the photogates such that the initial and final velocities of both the riders may be determined. *[Precaution: Keep the photogates as close to the point of collision as possible to minimize friction error.]*
4. Collide the two riders elastically using different initial conditions by varying the compression of the spring.
5. Replace the rubber band attachments with double-sided tape attachments (and counterweights) to simulate inelastic collisions.
6. Repeat steps 2-4.
7. In each case, verify the conservation of linear momentum and calculate the loss in kinetic energy and compare it to the theoretically expected value.

Observations

Part A

Length of interrupter card = $21.1 \pm 0.1 \text{ cm}$

Spring compression (cm)	Δt_1 (s)	Δt_2 (s)
3.0	0.516	0.524
2.7	0.582	0.593
2.5	0.607	0.619
2.2	0.752	0.776
2.0	0.818	0.855
1.7	0.981	1.037
1.5	1.183	1.295
1.2	1.620	1.876
1.0	2.293	3.144

Table 1: Time difference at each photogate for a rider released with varying amounts of spring compression

The raw data collected from the photogates can be found in the Appendix (Part A).

Part B

Length of Interrupter Card = $3.0 \pm 0.1 \text{ cm}$

Mass of the Rider = $207.0 \pm 0.1 \text{ g}$

Falling mass (g)	Δt_1 (s)	Δt_2 (s)
1.3	0.190	0.113
3.5	0.112	0.063
5.5	0.088	0.049
7.7	0.075	0.042
10.3	0.064	0.036
12.5	0.060	0.033
15.8	0.053	0.029

Table 2: Time difference at each photogate for a rider attached to different falling masses

The raw data collected from the photogates can be found in the Appendix (Part B).

Part C

Inelastic Collisions

Mass of rider a = $417.5 \pm 0.1 \text{ g}$

Mass of rider b = $234.6 \pm 0.1 \text{ g}$

Length of interrupter card of rider $a = 21.1 \pm 0.1 \text{ cm}$

Length of interrupter card of rider $b = 22.2 \pm 0.1 \text{ cm}$

Inelastic collisions keeping rider b at rest and giving rider a a push:

Δt_a (s)	$\Delta t'_{(a+b)}$ (s)
1.086	2.510
0.989	1.869
0.887	1.683
0.896	1.680
0.697	1.243
0.646	1.192
0.576	1.072

Table 3: Time difference data from two photogates for an inelastic collision where rider b is kept at rest and rider a is given a push

The raw data collected from the photogates can be found in the Appendix (Part C).

Inelastic collisions where both rider a and rider b are given a push:

Δt_a (s)	Δt_b (s)	$\Delta t'_{(a+b)}$ (s)
0.655	1.443	2.049
0.648	1.875	1.766
0.587	1.960	1.505
0.605	1.133	1.922
0.555	1.244	1.527
0.540	0.907	1.659
0.510	0.899	1.531

Table 4: Time difference data from two photogates for an inelastic collision where both rider a and rider b are given a push

The raw data collected from the photogates can be found in the Appendix (Part C).

Elastic Collisions

Mass of rider $a = 258.6 \pm 0.1 \text{ g}$

Mass of rider $b = 441.4 \pm 0.1 \text{ g}$

Length of interrupter card of rider $a = 22.2 \pm 0.1 \text{ cm}$

Length of interrupter card of rider $b = 21.1 \pm 0.1 \text{ cm}$

Elastic collisions keeping rider b at rest and giving rider a a push:

Δt_a (s)	$\Delta t'_a$ (s)	$\Delta t'_b$ (s)
0.905	3.803	1.259
0.788	3.241	1.085
0.663	2.765	0.893
0.615	2.598	0.826
0.548	2.235	0.739
0.507	1.989	0.685
0.515	2.205	0.690

Table 5: Time difference data from two photogates for an elastic collision where rider b is kept at rest and rider a is given a push

The raw data collected from the photogates can be found in the Appendix (Part C).

Elastic collisions where both rider a and rider b are given a push:

Δt_a (s)	Δt_b (s)	$\Delta t'_a$ (s)	$\Delta t'_b$ (s)
0.806	1.717	0.995	1.320
0.761	1.747	0.982	1.223
0.715	1.602	0.903	1.196
0.661	1.625	0.923	1.033
0.576	1.737	0.914	0.881
0.813	1.707	0.987	1.358
0.751	1.324	0.787	1.400

Table 6: Time difference data from two photogates for an elastic collision where both rider a and rider b are given a push

The raw data collected from the photogates can be found in the Appendix (Part C).

Analysis

Part A

Using the time difference data in table 1, we can find the average velocity over each Δt with $v_{avg} = \Delta x / \Delta t$, where Δx is the length of the interrupter card. This gives us the following velocities at each gate for each spring compression:

Spring compression (cm)	v_1 (cm/s)	v_2 (cm/s)	Δv (cm/s)
3.0	40.9	40.2	0.7
2.7	36.2	35.6	0.6
2.5	34.7	34.1	0.6
2.2	28.0	27.2	0.8
2.0	25.8	24.7	1.1
1.7	21.5	20.3	1.2
1.5	17.8	16.3	1.5
1.2	13.0	11.2	1.8
1.0	9.19	6.69	2.5

Table 7: Velocities at each photogate for a rider released with varying amounts of spring compression

Note that the velocity remains approximately constant between both photogates, with a difference in the order of 10^0 cm/s. Since the second velocity is consistently smaller than the first velocity, it is reasonable to assume that the energy loss is due to friction and drag forces acting on the body between the photogates. Low initial velocities are more sensitive to frictional error since damping forces are dependent on the velocity of a body.

If we plot the spring compression vs velocity, we can see that they appear to be linearly related:

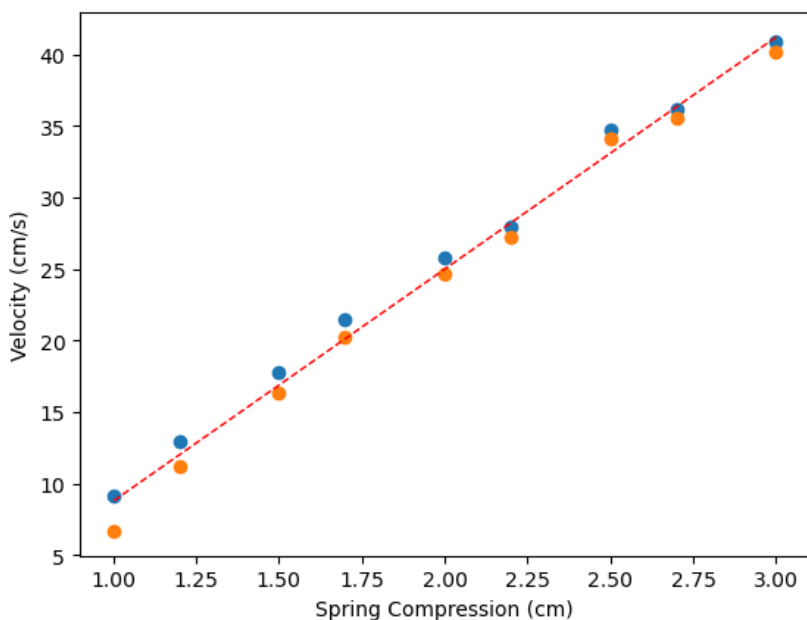


Figure 3: The velocity of the mass appears to be linearly related to the spring compression

This observation is in accordance with equation 1 which states that the velocity of a body pushed by a compressed spring is directly proportional to the compression of the spring:

$$v = x \sqrt{\frac{k}{m}}$$

Part B

From the time difference data in table 2, we can determine the velocity at each photogate using $v = \Delta x / \Delta t$. We can find the average acceleration between the two gates with $a = \Delta v / \Delta t'$, where $\Delta t'$ is the time difference between the two velocities. This gives us the following acceleration data for various falling masses:

Falling Mass (g)	v_1 (m/s)	v_2 (m/s)	Δv (m/s)	$\Delta t'$ (s)	a (m/s ²)
1.3	0.157	0.265	0.108	2.800	0.038
3.5	0.267	0.471	0.204	1.548	0.132
5.5	0.340	0.602	0.262	1.202	0.218
7.7	0.398	0.706	0.307	1.027	0.299
10.3	0.467	0.818	0.350	0.879	0.399
12.5	0.500	0.892	0.392	0.816	0.480
15.8	0.565	1.003	0.438	0.723	0.606

Table 8: Acceleration of the rider attached to various falling masses

Plotting the acceleration versus the mass of the falling object, we get the following graph:

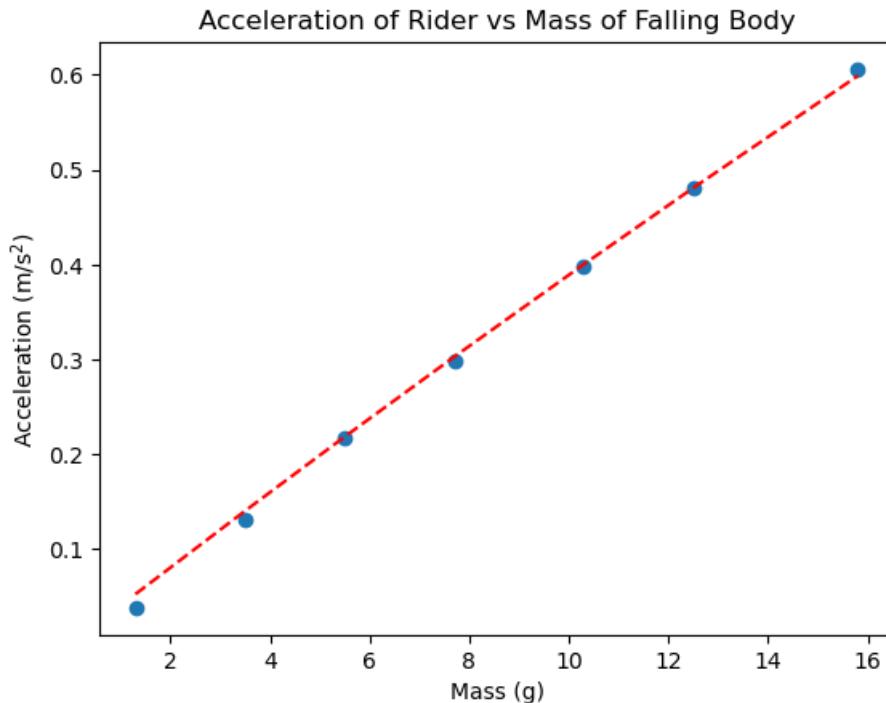


Figure 4: The graph appears to be nearly linear since $m \ll M$

We can curfit equation 2 onto this data to get a value of $g = 8.44 \text{ m/s}^2$. This shows that under a constant force, a body moves with a constant acceleration in accordance with Newton's second law.

Part C

Inelastic Collisions

From the time difference data in table 3 and the masses of both riders, we can determine the momentum and kinetic energy for each collision using the following formulas:

$$p = mv = m \frac{\Delta x}{\Delta t}$$

$$KE = \frac{1}{2}mv^2 = \frac{1}{2}m \left(\frac{\Delta x}{\Delta t} \right)^2$$

This data is represented in the following table:

p_a (g m/s)	$p'_{(a+b)}$ (g m/s)	KE_a (mJ)	$KE'_{(a+b)}$ (mJ)
81.1	57.7	7.87	2.55
89.0	77.4	9.49	4.60
99.3	86.0	11.8	5.67
98.3	86.2	11.6	5.69
126	116	19.1	10.4
136	121	22.2	11.3
153	135	28.0	14.0

Table 9: Momentum and kinetic energy for an inelastic collision where rider b is kept at rest and rider a is given a push

The momentum is nearly conserved, with an error upto 29%. This error is likely due to the effect of friction since higher velocities appear to have a lower error.

$$p_a \approx p'_{(a+b)}$$

The observed loss in kinetic energy is also greater than the expected loss in kinetic energy given by equation 4 for inelastic collisions. The difference between the observed and expected values are below:

$$\text{Observed } KE_{loss} = KE_a - KE'_{(a+b)}$$

$$\Delta KE_{loss} = \text{Observed } KE_{loss} - \text{Expected } KE_{loss}$$

Observed KE_{loss} (mJ)	Expected KE_{loss} (mJ)	ΔKE_{loss} (mJ)
5.32	2.83	2.49
4.89	3.41	1.48
6.13	4.24	1.89
5.87	4.16	1.71
8.73	6.88	1.85
10.9	8.00	2.93
14.0	10.0	4.00

Table 10: Difference between the observed and expected values of kinetic energy for an inelastic collision where rider b is kept at rest and rider a is given a push

Notice that the observed loss in kinetic energy is consistently greater than the expected result and is therefore most likely due to energy loss caused by friction and other damping forces. However, the difference in loss of kinetic energy does not appear to have any dependence on the velocity of the rider.

For an inelastic collision where both rider *a* and *b* are given a push, we get the following momentum and kinetic energy data:

p_a (g m/s)	p_b (g m/s)	$p'_{(a+b)}$ (g m/s)	KE_a (mJ)	KE_b (mJ)	$KE'_{(a+b)}$ (mJ)
134	-36.1	70.6	21.7	2.78	3.83
135	-27.8	82.0	22.1	1.64	5.15
149	-26.6	96.2	26.9	1.50	7.09
145	-46.0	75.3	25.4	4.50	4.35
158	-41.9	94.8	30.1	3.73	6.89
162	-57.4	87.3	31.8	7.02	5.84
172	-57.9	94.6	35.6	7.15	6.85

Table 11: Momentum and kinetic energy for an inelastic collision where both rider *a* and *b* are given a push

If we allow for error upto 29% in the momentum, we can assume that the momentum is conserved before and after the collision.

$$p_a + p_b \approx p'_{(a+b)}$$

The observed loss in kinetic energy and expected loss in kinetic energy from equation 4 for an inelastic collision of two moving masses is compared in the table below:

$$\text{Observed } KE_{loss} = (KE_a + KE_b) - KE'_{(a+b)}$$

$$\Delta KE_{loss} = \text{Observed } KE_{loss} - \text{Expected } KE_{loss}$$

Observed KE_{loss} (mJ)	Expected KE_{loss} (mJ)	ΔKE_{loss} (mJ)
20.6	17.0	3.6
18.6	14.8	3.8
20.4	20.0	0.4
19.6	19.6	0.0
16.9	16.6	0.3
21.3	16.7	4.6
25.5	22.3	3.2
26.9	23.4	3.5
29.6	23.1	6.5
32.9	30.3	2.6
35.9	32.7	3.2

Table 12: Difference between the observed and expected values of kinetic energy for an inelastic collision where both rider *a* and *b* are given a push

Once again, the observed loss in kinetic energy is consistently greater than the expected result and therefore is most likely due to energy loss caused by friction and other damping forces.

Elastic Collisions

For an elastic collision, we initially kept rider b at rest and gave rider a a push. Using the data in table 5, we can find the momentum and kinetic energy for these collisions:

p_a (g m/s)	p'_a (g m/s)	p'_b (g m/s)	KE_a (mJ)	KE'_a (mJ)	KE'_b (mJ)
63.4	-15.1	73.9	7.77	0.441	6.19
72.8	-17.7	85.8	10.3	0.606	8.34
86.5	-20.8	104.	14.5	0.833	12.3
93.3	-22.1	112.	16.8	0.944	14.4
104.6	-25.7	125.	21.2	1.275	18.0
113.2	-28.9	135.	24.8	1.610	20.9
111.3	-26.0	134.	24.0	1.310	20.6

Table 13: Momentum and kinetic energy for an elastic collision where rider b is kept at rest and rider a is given a push

In these collisions, momentum is conserved with an error margin of upto 8%. This is significantly better than the readings of inelastic collisions.

$$p_a \approx p'_a + p'_b$$

During a perfectly elastic collision there should be no loss of kinetic energy. However, since the system is imperfect, there is a small loss of kinetic energy which we can find by comparing the total initial and final kinetic energy of the system:

$$KE_{loss} = KE_a - (KE'_a + KE'_b)$$

KE_{loss} (mJ)
1.14
1.31
1.32
1.51
1.94
2.25
2.04

Table 14: Loss of kinetic energy in an imperfectly elastic collision where rider b is kept at rest and rider a is given a push

This observed loss in kinetic energy is likely due to damping forces acting on both bodies. Furthermore, since we used rubber bands for the elastic collision, there is energy lost during the contact of the two bands and the collision is imperfectly elastic.

When both rider *a* and rider *b* are given a push and made to collide elastically, we get the following momentum and kinetic energy from the data in table 6.

p_a (g m/s)	p_b (g m/s)	p'_a (g m/s)	p'_b (g m/s)	KE_a (mJ)	KE_b (mJ)	KE'_a (mJ)	KE'_b (mJ)
71.2	-54.2	-57.7	70.5	9.80	3.33	6.43	5.64
75.4	-53.3	-58.4	76.1	11.0	3.22	6.60	6.57
80.2	-58.1	-63.6	77.8	12.4	3.83	7.81	6.86
86.8	-57.3	-62.1	90.1	14.6	3.72	7.47	9.20
99.6	-53.6	-62.8	105.7	19.2	3.25	7.62	12.6
70.6	-54.6	-58.1	68.5	9.63	3.37	6.54	5.32
76.4	-70.3	-72.9	66.5	11.3	5.60	10.3	5.01

Table 15: Momentum and kinetic energy for an elastic collision where both rider *a* and rider *b* are given a push

If we allow for an error of upto 35%, we can assume that the momentum is conserved. However, such a high error is clearly not acceptable and is indicative of the large amount of friction present in the system.

$$p_a + p_b \approx p'_a + p'_b$$

Due to the same frictional forces, there is also a loss in the total kinetic energy before and after the elastic collision.

$$KE_{loss} = (KE_a + KE_b) - (KE'_a + KE'_b)$$

KE_{loss} (mJ)
1.06
1.05
1.59
1.63
2.17
1.14
1.60

Table 16: Loss of kinetic energy in an imperfectly elastic collision where both rider *a* and rider *b* are given a push

This roughly consistent loss of kinetic energy indicates that it is due to an inherent loss of energy in the system itself, likely due to the imperfect nature of the collision and the friction on the track.

Error Analysis

The error in the velocity data in part A comes from the error in the measurement of Δx and Δt . These measurements have a least count error of $\delta x = 0.1$ cm and $\delta t = 2 \times 10^{-6}$ s.

$$\delta v = v \left(\frac{\delta x}{\Delta x} + \frac{\delta t}{\Delta t} \right)$$

Using the above formula we can find an error bar δv for every velocity reading, and a total error margin of $\delta v_1 + \delta v_2$ for every pair of velocities. If $\Delta v = v_1 - v_2$ lies within this margin, we can assume that the velocity remains constant in accordance with Netwon's first law.

δv_1 (cm/s)	δv_2 (cm/s)	$\delta v_1 + \delta v_2$ (cm/s)	Δv (cm/s)
0.194	0.191	0.385	0.7
0.172	0.169	0.34	0.6
0.165	0.162	0.326	0.6
0.133	0.129	0.262	0.8
0.122	0.117	0.239	1.1
0.102	0.096	0.198	1.2
0.084	0.077	0.162	1.5
0.062	0.053	0.115	1.8
0.044	0.032	0.075	2.5

Table 17: Calculated error margin $\delta v_1 + \delta v_2$ vs observed error Δv

Clearly, the observed error is larger than the calculated error. This is most likely due to frictional forces that have not been accounted for in this calculation. This hypothesis is strengthened by the fact that the error increases for lower velocities which are more sensitive to frictional slowing.

In part B, we can calculate the error in the acceleration by a similar method:

$$\delta a = a \left(\frac{\delta v}{\Delta v} + \frac{\delta t'}{\Delta t'} \right)$$

Here, $\delta t = 2 \times 10^{-6}$ and $\delta v = \delta v_1 + \delta v_2$ as calculated in the last part.

a (m/s ²)	δa (m/s ²)
0.038	0.00503
0.132	0.0159
0.218	0.0261
0.299	0.0359
0.399	0.0488
0.480	0.0570
0.606	0.0724

Table 18: Calculated error margin δa for the acceleration of the rider attached to a falling mass

This gives us a maximum and minimum range of accelerations which correspondingly give us a maximum and minimum value of g .

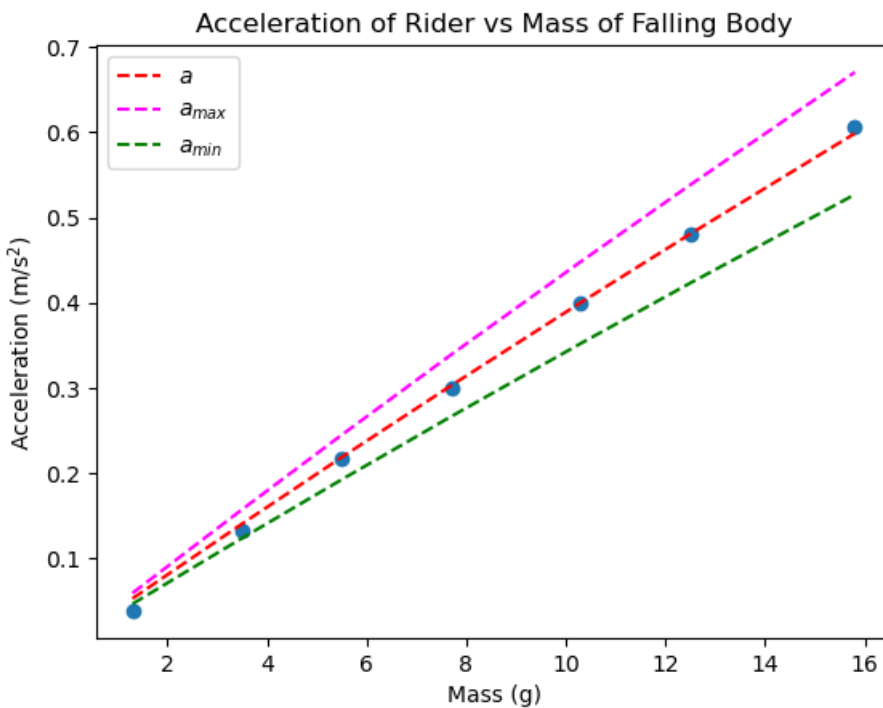


Figure 5: Error margin for acceleration versus mass

This gives us $g_{max} = 9.46 \text{ m/s}^2$ and $g_{min} = 7.43 \text{ m/s}^2$. The reason the true value of g may not fall in this range is due to the frictional forces not accounted for.

Results

Part A

The velocity of a body remains constant when no external forces are applied on it in accordance with Newton's first law.

The velocity of a body released by a compressed spring is proportional to the compression of the spring.

$$v = x \sqrt{\frac{k}{m}}$$

Part B

A rider experiencing a constant force from a falling mass undergoes constant acceleration in accordance with Newton's second law.

We can find a value of $g = 8.45 \pm 1.02 \text{ m/s}^2$.

Part C

The momentum of two colliding riders (both elastic and inelastic), tends to be conserved before and after the collision. However, there is significant error which is assumed to be due to frictional and damping forces.

The kinetic energy loss is also greater than the theoretically expected results due to energy lost to friction and heat.

Appendix

Part A

Spring compression (cm)	$T_i(1)$ (s)	$T_f(1)$ (s)	$T_i(2)$ (s)	$T_f(2)$ (s)
3.0	1.065983	1.582435	1.79525	2.319514
2.7	10.336242	10.918725	11.159431	11.752949
2.5	3.02392	3.631572	3.882888	4.502289
2.2	0.204723	0.957496	1.269174	2.045939
2.0	1.731706	2.54992	2.890749	3.746013
1.7	1.641889	2.623022	3.03548	4.073202
1.5	2.13661	3.319836	3.828302	5.12366
1.2	2.288943	3.909822	4.63134	6.507529
1.0	1.654648	3.948465	5.088422	8.23327

Table 19: Time data collected from two vernier photogates for a rider released with varying amounts of spring compression

Part B

Falling mass (g)	$T_i(1)$ (s)	$T_f(1)$ (s)	$T_i(2)$ (s)	$T_f(2)$ (s)
1.3	2.602328	2.793119	5.440638	5.553937
3.5	4.299777	4.412091	5.872243	5.935942
5.5	1.940624	2.028871	3.162134	3.211999
7.7	1.634496	1.709798	2.677928	2.720445
10.3	2.246882	2.311085	3.139631	3.176321
12.5	1.173633	1.233633	2.002722	2.036356
15.8	2.485243	2.538348	3.219393	3.249314

Table 20: Time data collected from two vernier photogates for a rider attached to different falling masses

Part C

Inelastic Collisions

$T_i(a)$ (s)	$T_f(a)$ (s)	$T'_i(a + b)$ (s)	$T'_f(a + b)$ (s)
9.281719	10.368324	13.798669	16.308804
5.042178	6.031781	9.01809	10.887488
11.10028	11.987905	14.712669	16.396356
12.38207	13.278708	16.038779	17.719211
9.056596	9.7538	11.883447	13.12691
13.060327	13.707002	15.707685	16.900263
2.988369	3.564795	5.353003	6.425059

Table 21: Time data collected from two vernier photogates for an inelastic collision where rider b is kept at rest and rider a is given a push

$T_i(a)$ (s)	$T_f(a)$ (s)	$T_i(b)$ (s)	$T_f(b)$ (s)	$T'_i(a + b)$ (s)	$T'_f(a + b)$ (s)
9.747059	10.402083	8.999732	10.44286	11.448053	13.49745
4.501911	5.150813	3.865469	5.740622	5.883897	7.650363
6.131493	6.719265	4.904653	6.865258	7.491155	8.99624
6.151532	6.756773	5.975025	7.108208	7.871543	9.794129
14.350181	14.9058	13.765367	15.009821	15.696089	17.223307
6.614782	7.155635	6.153456	7.061064	8.179477	9.838629
6.893958	7.404918	6.366907	7.266166	8.387361	9.918448

Table 22: Time data collected from two vernier photogates for an inelastic collision where both rider a and rider b are given a push

Elastic Collisions

$T_i(a)$ (s)	$T_f(a)$ (s)	$T'_i(a)$ (s)	$T'_f(a)$ (s)	$T'_i(b)$ (s)	$T'_f(b)$ (s)
9.999799	10.905546	12.012476	15.815691	11.850301	13.110254
6.231808	7.020173	8.173243	11.415012	7.882951	8.96843
8.087187	8.751036	9.777975	12.543752	9.449736	10.343423
5.504819	6.120244	7.10056	9.699117	6.774831	7.601723
4.684534	5.233159	6.130473	8.36629	5.829063	6.568803
5.129665	5.63691	6.482322	8.471863	6.196244	6.881835
4.26091	4.776601	5.661115	7.866497	5.339617	6.029984

Table 23: Time data collected from two vernier photogates for an elastic collision where rider b is kept at rest and rider a is given a push

$T_i(a)$ (s)	$T_f(a)$ (s)	$T_i(b)$ (s)	$T_f(b)$ (s)	$T'_i(a)$ (s)	$T'_f(a)$ (s)	$T'_i(b)$ (s)	$T'_f(b)$ (s)
4.744508	5.55102	3.636424	5.353968	6.49364	7.488785	6.453858	7.774267
4.230413	4.99172	3.038547	4.785894	5.930577	6.913363	5.833575	7.056741
5.566572	6.282411	4.180913	5.783584	6.943377	7.846688	7.165761	8.362479
3.978261	4.639289	2.976897	4.602514	5.637874	6.561663	5.343518	6.376771
4.947432	5.52382	4.179213	5.916735	6.803638	7.717952	6.067509	6.948998
3.683678	4.497269	2.571036	4.278075	5.424571	6.41189	5.421224	6.779886
3.590303	4.341552	2.453039	3.778016	4.814791	5.602416	5.399649	6.799798

Table 24: Time data collected from two vernier photogates for an elastic collision where both rider a and rider b are given a push